Journal of Cranio-Maxillo-Facial Surgery 47 (2019) 1464–1474

Contents lists available at ScienceDirect

Journal of Cranio-Maxillo-Facial Surgery

journal homepage: www.jcmfs.com

Gingival fibroblasts and medication-related osteonecrosis of the jaw: Results by real-time and wound healing in vitro assays

Anna Yuan*, Adelheid Munz, Siegmar Reinert, Sebastian Hoefert

Department of Oral and Maxillofacial Surgery, University Hospital Tuebingen, Osianderstr 2-8, 72076, Tübingen, Germany

ARTICLE INFO

Article history:
Paper received 5 March 2019
Accepted 2 June 2019
Available online 8 June 2019

Keywords:
Osteonecrosis
Bisphosphonates
Denosumab
Fibroblasts

ABSTRACT

Objective: This study investigated the effects of bisphosphonates and denosumab on human gingival fibroblasts (HGFs) that could influence inflammation, wound healing, and angiogenesis in medication-related osteonecrosis of the jaw (MRONJ).

Methods: A real-time *in vitro* assay was performed on HGFs with and without the addition of bacterial lipopolysaccharide and a mononuclear cell co-culture to observe the effects of zoledronate, ibandronate, alendronate, clodronate, denosumab, and combinations of zoledronate and denosumab at varied concentrations. A wound healing assay was performed, and gene and protein expression was analyzed for inflammatory, angiogenic, and osteoclastogenic cytokines and mediators including interleukin (IL)-1β, IL-6, tumor necrosis factor alpha (TNFα), IL-8, vascular endothelial growth factor (VEGF), RANKL, and osteoprotegerin.

Results: Higher concentrations of antiresorptives resulted in impaired wound healing and HGF death, which also occurred without mechanical damage. These effects were increased with bacterial lipopolysaccharide and mononuclear cells. Increased levels of IL-1β, TNFα, IL-8, VEGF, osteoprotegerin, and decreased levels of IL-6 were observed.

Conclusions: Antiresorptive exposure was associated with HGF death and delayed wound healing, which could be attributed to an elevated inflammatory response and immune dysfunction contributing to MRONJ development. There was no evidence of anti-angiogenic effects. Our experiments present the first results of denosumab with HGFs.

1. Introduction

Antiresorptive drugs such as bisphosphonates (BPs) and the receptor activator of nuclear factor kappa-B ligand (RANKL)-inhibitor denosumab are used for the treatment of osteoporosis, Paget's disease, hypercalcemia of malignancy, multiple myeloma, and metastatic bone disease (Ruggiero et al., 2014). Medication-related osteonecrosis of the jaw (MRONJ) is a serious complication of these frequently prescribed medications. Although the first case of bisphosphonate-related osteonecrosis of the jaw (BRONJ) was reported in 2003 (Marx, 2003), the pathogenesis of the disease remains unclear. Treatment of MRONJ is difficult and costly, and has an enormous impact on patients' quality of life.

Various mechanisms have been proposed for the pathogenesis of MRONJ, one of which involves soft tissue toxicity (Scheper et al., 2010). Although the loss of the mucosa covering bone is the primary clinical feature of MRONJ (Reid et al., 2007), the role of soft tissue in pathogenesis is particularly not well defined. Some authors propose that soft tissues exposed to BPs could allow for bacterial ingress or trigger an inflammatory reaction, which could be exacerbated by the effect of BPs released from bone. HGFs have been previously analysed in vitro at arbitrarily determined time points (Scheper et al., 2009; Acil et al., 2012), but no real-time analysis has been performed. Furthermore, the involvement of denosumab in oral soft tissue toxicity has not yet been investigated.

This study aimed to investigate the role of antiresorptives in soft tissue cell death using a HGF model in real-time to assess cellular growth, viability, and cytotoxicity in cell culture(Hoefert et al., 2016). We analyzed if this effect was dose-dependent and

* Corresponding author. Tufts University School of Dental Medicine, Division of Oral Medicine, 1 Kneeland St., Boston, MA, 02111, USA. Fax: +1617 636 3657.
E-mail addresses: anna.yuan@tufts.edu (A. Yuan), adelheid.munz@med.uni-tuebingen.de (A. Munz), Siegmar.Reinert@med.uni-tuebingen.de (S. Reinert), sebastian.hoefert@uni-tuebingen.de (S. Hoefert).

https://doi.org/10.1016/j.jcms.2019.06.004
1010-5182/

observed the influence of a bacterial challenge simulated by lipopolysaccharide (LPS) and the consequences on wound healing. A further co-culture of mononuclear cells with HGFs allowed for the observation of immunologic effects such as the secretion of mediators or growth factors reported with periodontitis (Suthin et al., 2003; Baek et al., 2013). Gene expression and cytokine analyses were performed for markers of inflammation, angiogenesis, and osteoclastogenesis.

2. Materials and methods

2.1. Cell culture

Commercially available HGFs (Provitro, Berlin, Germany) were cultured in HGF medium (Provitro, Berlin, Germany). THP-1 human monocytic cells (ATCC, Manassas, VA, USA) were cultured in RPMI-1640 medium (GIBCO, Darmstadt, Germany). Cells were cultured in 75 cm^2 flasks at 37°C in a humidified incubator at 5% CO_2. Subculturing was performed when HGF confluence exceeded 75% and THP-1 cell density exceeded 5 to 7 $\times$ 10^6.

2.2. Real-time analysis

Using the xCELLigence® E-plates 16 and E-plates 16 VIEW (ACEA Biosciences Inc., San Diego, USA) for continuous monitoring of cell adherence, changes of impedance for cells attached to the detector plates were measured at 20 mV every 15 min and calculated as the dimensionless parameter Cell Index (CI):

$$CI = [Z_i - Z_0]/15$$

[Z_i: impedance at an individual experimental point; Z_0: background measurement at the beginning of the experiment].

Figures were displayed with the Delta Cell Index (DCI_{ti}), a standardized calculation of Cell Index (CI_{ti}) using a constant (delta value) over time with standard deviation. The measured value was proportional to the number of attached cells to the detector plate and quality of attachment. The optimal HGF growth curve was determined. Live monitoring was performed for a minimum of 216 h. The mean of the inflexion point of cell adherence indicating the beginning of cell death predominance was calculated from live-monitoring data for each concentration. Intraindividual differences of inflexion points of adherence to the maximum control value in each experiment set were also calculated to exclude individual experiment bias. Each experiment was performed in duplicates and repeated at least twice to confirm reproducibility of results.

Zoledronate (Sequoia Research Products, Pangbourne, UK), ibandronate (Sigma-Aldrich, Taufkirchen, Germany) and alendronate (Sequoia Research Products, Pangbourne, UK) 0.5 μM, 5 μM, and 50 μM(Reid et al., 2007; Landesberg et al., 2008; Soydan et al., 2015); clodronate (Sigma-Aldrich, Taufkirchen, Germany) 50 μM, 125 μM, and 500 μM(Walter et al., 2008); denosumab 3 μg/mL, 10 μg/mL, and 40 μg/mL (Bekker et al., 2004); or a combination of zoledronate and denosumab in the concentrations of 0.5 μM + 40 μg/mL, 5 μM + 10 μg/mL, and 5 μM + 40 μg/mL were added to each E-plate well containing HGFs according to concentrations established in literature (Scheper et al., 2009; Komatsu et al., 2016). Porphyromonas gingivalis (P. gingivalis) LPS (InvivoGen, San Diego, USA) 10 μg/mL was added with BP at 48 h. In the co-culture, BPs, LPS 10 μg/mL, and THP-1 cell suspension in RPMI medium were added to the E-plate insert (ACEA Biosciences Inc., San Diego, USA) at 48 h and loaded onto the E-plate. The E-plate insert allowed for two cell populations to be separated by a 0.4 μm pore membrane, enabling the measurement of indirect cell-to-cell interactions.

2.3. Wound healing assays

Real-time experiments were confirmed in 24-well plates (Costar, Kaiserslautern, Germany) with antiresorptives only, antiresorptives and LPS, and a co-culture with antiresorptives, LPS, and THP-1 cells. One plate with a scratch assay and one without were used for each experiment set to assess wound healing. Confluent cell layers were scraped at 48 h with a 200 μL pipette tip, and antiresorptives were added. In LPS experiments, P. gingivalis LPS 10 μg/mL was added with antiresorptives during the 48 h medium change. For co-culture experiments, a THP-1 cell suspension and LPS 10 μg/mL were added into a Greiner ThinCert™ (Greiner Bio-One, Frickenhausen, Germany) with the same 0.4 μm pore membrane. Experiments were run for 9 days for the antiresorptive and LPS experiments, and 6 days for the co-culture. Each experiment was performed in duplicates and repeated at least twice. Cells were visualized by inverted light microscopy (Leica Microsystems, Wetzlar, Germany), and digital images were collected.

2.4. Gene expression analysis

HGFs were collected after 24 h of antiresorptive treatment with and without LPS. Wells were washed with PBS, incubated with 80 μL trypsin, and centrifuged. The supernatant was removed and 100 μL RA1 Buffer with 2 μL TCEP (NucleoSpin RNA XS, Macherey-Nagel, Düren, Germany) was added. Highly pure RNA was isolated using the NucleoSpin RNA XS (Macherey-Nagel, Düren, Germany) and measured with a Qubit 3.0 Fluorometer (Thermo Fisher Scientific, Waltham, USA). Single-strand cDNA was synthesized using 70–116 ng/μL of total RNA using an oligo-dT primer (Advantage RT-for-PCR Kit; Clontech, Heidelberg, Germany). Primers for tumor necrosis factor alpha (TNFα), interleukin (IL)-8, osteoprotegerin (OPG), RANKL, and glyceraldehyde-3-phosphate dehydrogenase (GAPDH) were obtained from the LightCycler Primer Set (Search LC, Heidelberg, Germany). Each cDNA was amplified in the presence of SYBR Green Master Mix. The quantification of GAPDH encoding messenger RNA (mRNA) served as an internal control for each cDNA sample. The conditions for PCR were 1 $\times$ (95 °C, 10 min) denaturation, 40 $\times$ (95 °C, 10 s; 68 °C, 10 s; 72 °C, 16 s) amplification, 1 $\times$ (95 °C, 1 s; 58 °C, 10 s; 95 °C, 1 s) melting curve, and 1 $\times$ (40 °C, 30 s) cooling. Gene expression analysis was performed with the Light Cycler 2.0 System (Roche, Basel, Switzerland).

2.5. Protein expression analysis

Cell culture supernatant was collected from co-culture at 24 and 96 h. The production of IL-1β, VEGF, and IL-6 was measured using the Human IL-1β Quantikine ELISA Immunoassay (R&D Systems, Minneapolis, USA), the Human VEGF Quantikine ELISA Immunoassay (R&D Systems, Minneapolis, USA), and a Human IL-6 Quantikine ELISA Immunoassay (R&D Systems, Minneapolis, USA). The absorbance values of IL-1β, VEGF, and IL-6 secretion were measured at wavelengths of 450 nm, with corrections of 540 nm or 570 nm. Protein expression analysis was performed by the ELISA reader (BioTek, Winooski, USA).

2.6. Statistical analysis

Statistical analyses were performed using RTCA Software 1.2.1 (ACEA Biosciences Inc., San Diego, USA) and JMP 10.0.2 (SAS Institute, Cary, NC, USA). The primary outcomes were the inflexion points of cell adherence and calculated concentrations or relative gene expression in the ELISA and qPCR analyses. Intraindividual differences of inflexion points to the individual experiment control were calculated to account for experiment set bias. A paired

Student's t-test was performed, and the Tukey-Kramer method was used to confirm results and account for experiment–wise error. A p value < .05 was significant.

3. Results

3.1. Real-time analysis

Live monitoring indicated a similar initial differentiation of treated and untreated HGFs for 60 h (Fig. 1), followed by an individual inflexion point of adherence. The inflexion point for the control was observed after 90.4 h. Nitrogen-containing BPs at 50 μM exhibited inflexion points from 64.0 ± 1.0 (alendronate) to 66.0 ± 4.2 h (zoledronate), with later inflexion points for denosumab (69.5 ± 0.7 h), the combination of zoledronate and denosumab (70.0 ± 1.0 h), and non-nitrogen-containing clodronate (78.0 ± 6.9 h). Differences to control were significant with 50 μM alendronate. Intraindividual differences to the control in each experiment set exhibited a significance to the control at concentrations of 50 μM for zoledronate (−22.5 h), alendronate (−27.7 h), and ibandronate (−22.0 h), as well for the combination of 5 μM zoledronate + 10 μg/mL denosumab (20.3 h).

For HGFs treated with antiresorptives and P. gingivalis LPS, a similar initial differentiation was observed for 60 h (Fig. 2). The inflexion point of adherence for the control was observed after 125.3 h, and for the control with LPS after 105.2 ± 12.0 h. Nitrogen-containing BPs at 50 μM exhibited inflexion points from 63.0 ± 4.4 h (zoledronate) to 78.0 ± 18.3 h (ibandronate), with later inflexion points for non-nitrogen BP clodronate (89.0 ± 2.8 h) and denosumab and the combination of zoledronate and denosumab (both 117.0 ± 16.9 h). Differences to control were significant with 50 μM zoledronate, 50 μM ibandronate, and all concentrations of alendronate dose-dependently. Intraindividual differences of the inflexion points in each experiment set exhibited a significance to the maximum control value at concentrations of 50 μM for zoledronate (−93.5 h) and all concentrations of alendronate dose-dependently.

For HGFs treated with antiresorptives and LPS in co-culture with THP-1 cells, a similar initial differentiation was observed for 50 h (Fig. 3). The inflexion point of adherence for the control was observed after 149.6 ± 8.6 h. Nitrogen-containing BPs at 50 μM exhibited inflexion points from 57.6 ± 9.8 h (zoledronate) to 68.0 ± 4.2 h (ibandronate), with later inflexion points for the combination of zoledronate and denosumab (101.0 ± 67.8 h), denosumab (152.0 ± 4.2 h), and clodronate (155.0 ± 9.9 h). Differences to control were significant with 50 μM alendronate, 50 μM ibandronate, the combination of 5 μM zoledronate +40 μg/mL denosumab, and zoledronate 50 μM and 5 μM dose-dependently. Intraindividual differences of the inflexion points exhibited a significance to the maximum control value for 50 μM alendronate (−90.0 h) and ibandronate (−82.5 h), the combination of 5 μM zoledronate + 40 μg/mL denosumab (−44.0 h), and zoledronate 50 μM and 5 μM dose-dependently.

3.2. Wound healing assays

Effects on wound healing were observed between 72 and 96 h in clodronate 500 μM, ibandronate 5 μM and 50 μM, alendronate 50 μM, zoledronate 5 μM + denosumab 10 μg/mL, and zoledronate 5 μM, with severe fibroblast death in zoledronate 50 μM (Fig. 4). By 168 h, ibandronate 50 μM, zoledronate 50 μM, zoledronate 5 μM + denosumab 10 μg/mL, alendronate 50 μM demonstrated severe cell death, while clodronate 500 μM showed mild signs of cell death compared to confluent controls. Fibroblasts exposed to P. gingivalis LPS with antiresorptives demonstrated further delayed wound healing. Zoledronate 50 μM exhibited signs of cell death as early as 24 h. By 48 h, wound healing was affected in clodronate 500 μM, denosumab 40 μg/mL, ibandronate 5 μM and 50 μM, zoledronate 0.5 μM and 5 μM, zoledronate 5 μM + denosumab 10 μg/mL, alendronate 50 μM, with zoledronate 50 μM having progressed to severe cell death. By 96 h, both alendronate 50 μM and zoledronate 50 μM exhibited severe cell death.

Antiresorptives were toxic to HGF in the 24-well plates without mechanical damage (Fig. 5). Cells exposed to zoledronate 50 μM appeared apoptotic at 24 h after antiresorptive addition. By 168 h, ibandronate 50 μM, zoledronate 50 μM, zoledronate 5 μM + denosumab 10 μg/mL, alendronate 50 μM demonstrated severe cell death. In plates exposed to antiresorptive and LPS, zoledronate 50 μM demonstrated similar early cell death, with alendronate 50 μM also appearing apoptotic at 96 h. Findings were analogous to the inflexion points of adherence observed in real-time experiments.

3.3. Gene and protein expression analysis

High concentrations of zoledronate with LPS demonstrated a 16-fold upregulation in mRNA expression of IL-8 in HGFs compared to controls (Fig. 6). Zoledronate 50 μM (and slightly denosumab 40 μg/mL) with LPS upregulated mRNA expression of TNFα in HGFs by 443-fold and 2.66-fold, respectively, as well as increased OPG expression (zoledronate: 773-fold; denosumab: 6.01-fold) compared to controls. The expression of RANKL by HGF was only slightly elevated by zoledronate 50 μM with LPS (2.49-fold). All antiresorptives significantly increased the expression of IL-1β in both the scratch and non-scratch assay compared to controls (Fig. 7). In contrast, IL-6 levels were significantly decreased in HGFs exposed to 50 μM nitrogen-containing BPs. For VEGF, all antiresorptives elevated the expression of VEGF compared to the control; this was statistically significant with the exception of clodronate.

4. Discussion

The loss of soft tissue remains the primary clinical feature of MRONJ, since exposed bone is a criterion for almost all stages of the disease by definition. Therefore, the inability of the mucosa to heal plays a key role in the etiology and clinical presentation, which may be influenced by the type of antiresorptive as well as by the presence of infection. There have been a handful of studies on HGFs with toxicity (Scheper et al., 2010; Walter et al., 2010, 2011; Cozin et al., 2011; Mawardi et al., 2011; Ravosa et al., 2011) and decreased collagen production demonstrated with alendronate, zoledronate, and pamidronate (Acil et al., 2012). Apoptosis and inhibited cellular proliferation with 1–100 μM of zoledronate on HGFs were observed to increase with concentration and time (Fu et al., 2015; Soydan et al., 2015). We observed significantly earlier HGF death with high concentrations of nitrogen-containing BPs, with lower concentrations affected with the introduction of LPS and THP-1 cells.

Nitrogen-containing BPs are not metabolized and accumulate in the bone, whereas non-nitrogen containing BPs are rapidly excreted by the kidneys (Monkkonen et al., 1990). Nitrogen-containing BPs inhibit farnesyl disphosphate synthase in the mevalonate pathway (Cozin et al., 2011). There has been evidence of suppressed epithelial cell growth by nitrogen-containing BPs via inhibition of the mevalonate pathway and a subsequent reduction in geranylgeraniol synthesis (Zafar et al., 2014). Geranylgeraniol is necessary for membrane localization of intracellular proteins, including caspase 3, a main regulator of cellular apoptosis, and the

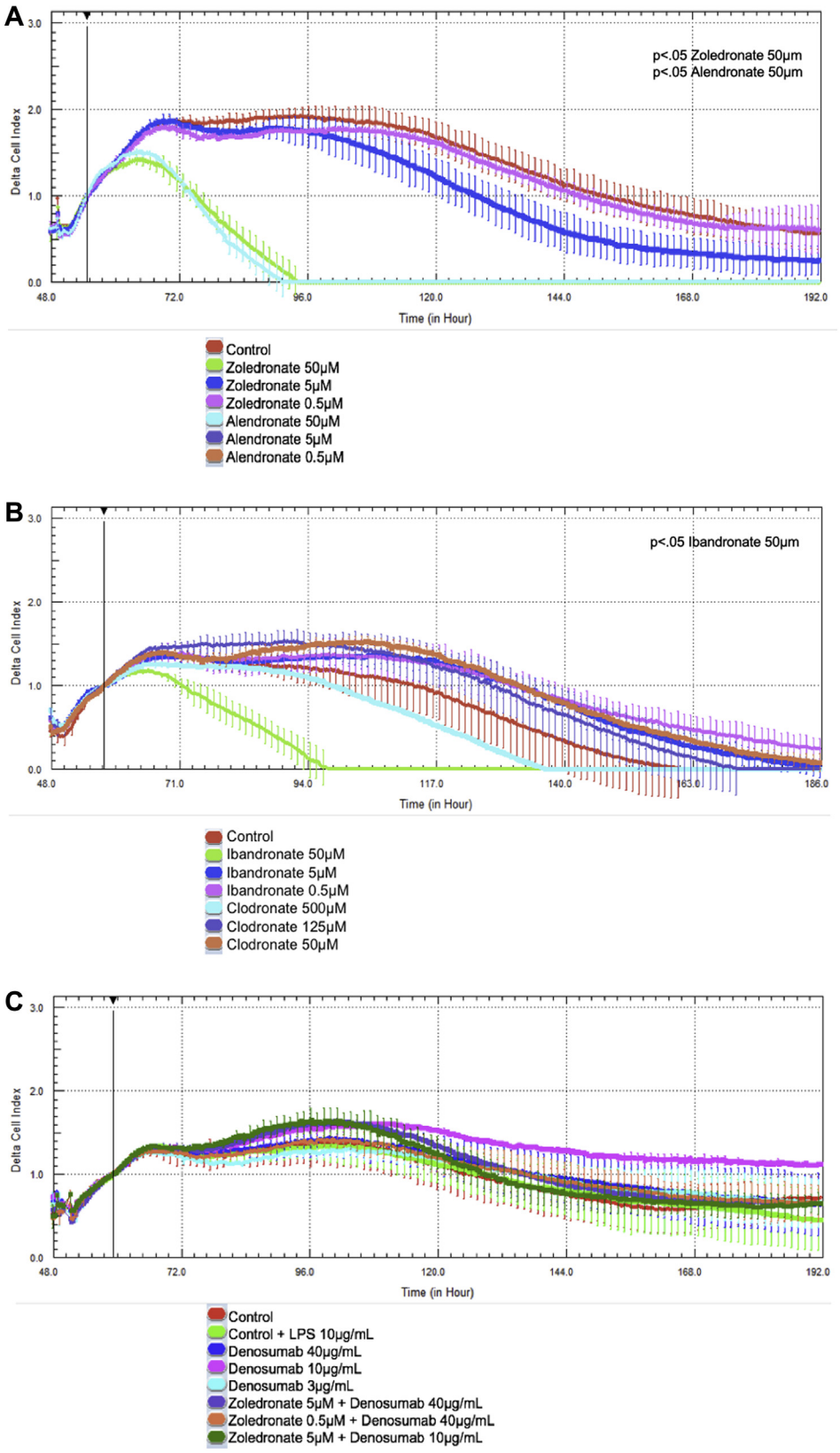

Fig. 1. Real-time monitoring of human gingival fibroblast cell adherence after confluence and exposure to antiresorptive medications at various concentrations. Cell curve describes the mean values of cell impedance and standard deviation up to 190 h of observation for the adherence curves of controls and (A) zoledronate and alendronate at concentrations of 0.5 µM, 5 µM, and 50 µM (B) clodronate at concentrations of 50 µM, 125 µM, and 500 µM and ibandronate at concentrations of 0.5 µM, 5 µM, and 50 µM, (C) denosumab at concentrations of 3 µg/mL, 10 µg/mL, and 40 µg/mL and combination of zoledronate and denosumab at concentrations of zoledronate 5 µM + denosumab 40 µg/mL, zoledronate 0.5 µM + denosumab 40 µg/mL, and zoledronate 5 µM + denosumab 10 µg/mL. Curve interruption is caused by medium renewal.

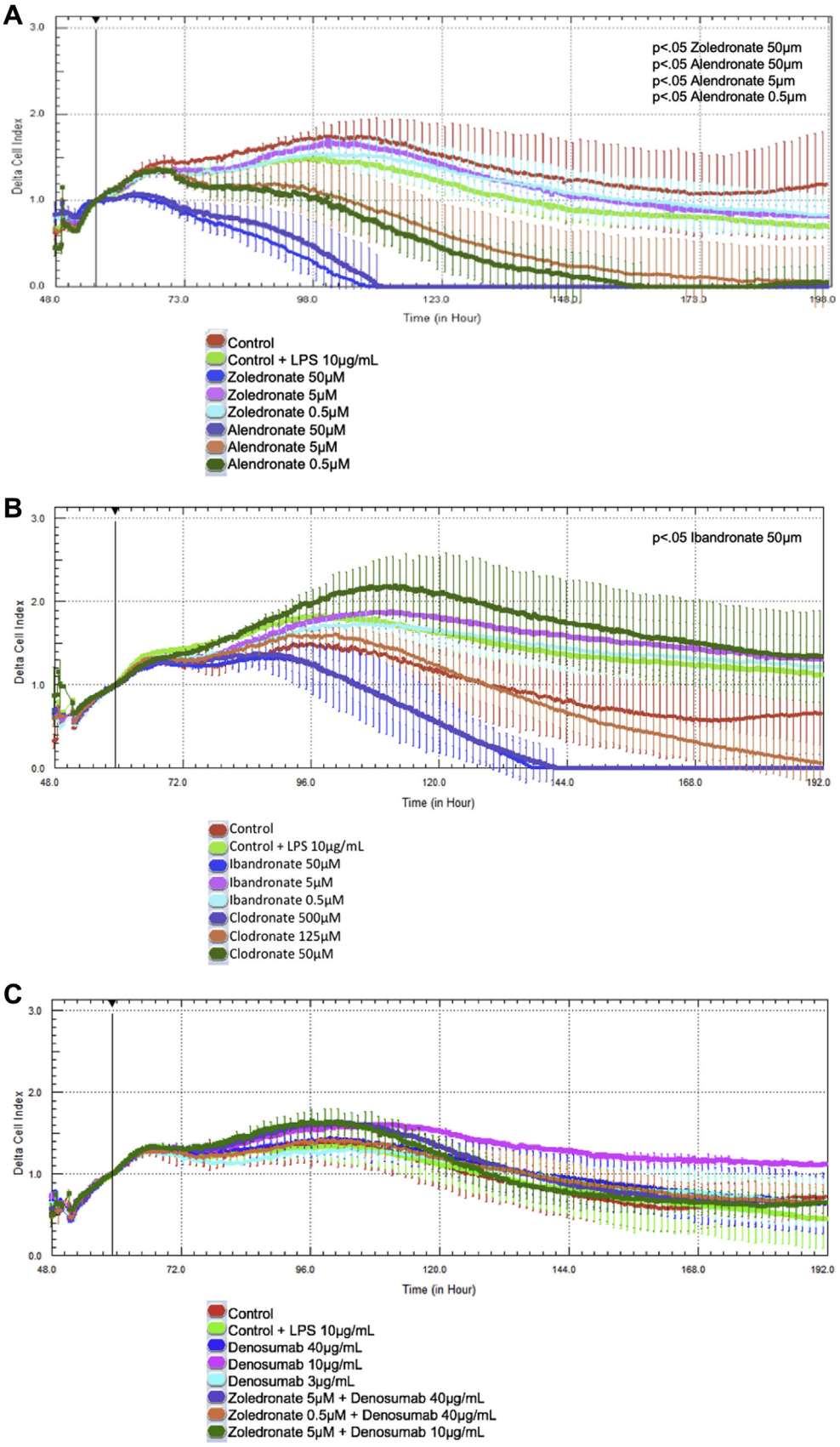

Fig. 2. Real-time monitoring of human gingival fibroblast cell adherence after confluence and exposure to Porphyromonas gingivalis lipopolysaccharide 10 µg/mL and antiresorptive medications at various concentrations. Cell curve describes the mean values of cell impedance and standard deviation up to 190 h of observation for the adherence curves of controls and (A) zoledronate and alendronate at concentrations of 0.5 µM, 5 µM, and 50 µM (B) clodronate at concentrations of 50 µM, 125 µM, and 500 µM and ibandronate at concentrations of 0.5 µM, 5 µM, and 50 µM, (C) denosumab at concentrations of 3 µg/mL, 10 µg/mL, and 40 µg/mL and combination of zoledronate and denosumab at concentrations of zoledronate 5 µM + denosumab 40 µg/mL, zoledronate 0.5 µM + denosumab 40 µg/mL, and zoledronate 5 µM + denosumab 10 µg/mL. Curve interruption is caused by medium renewal.

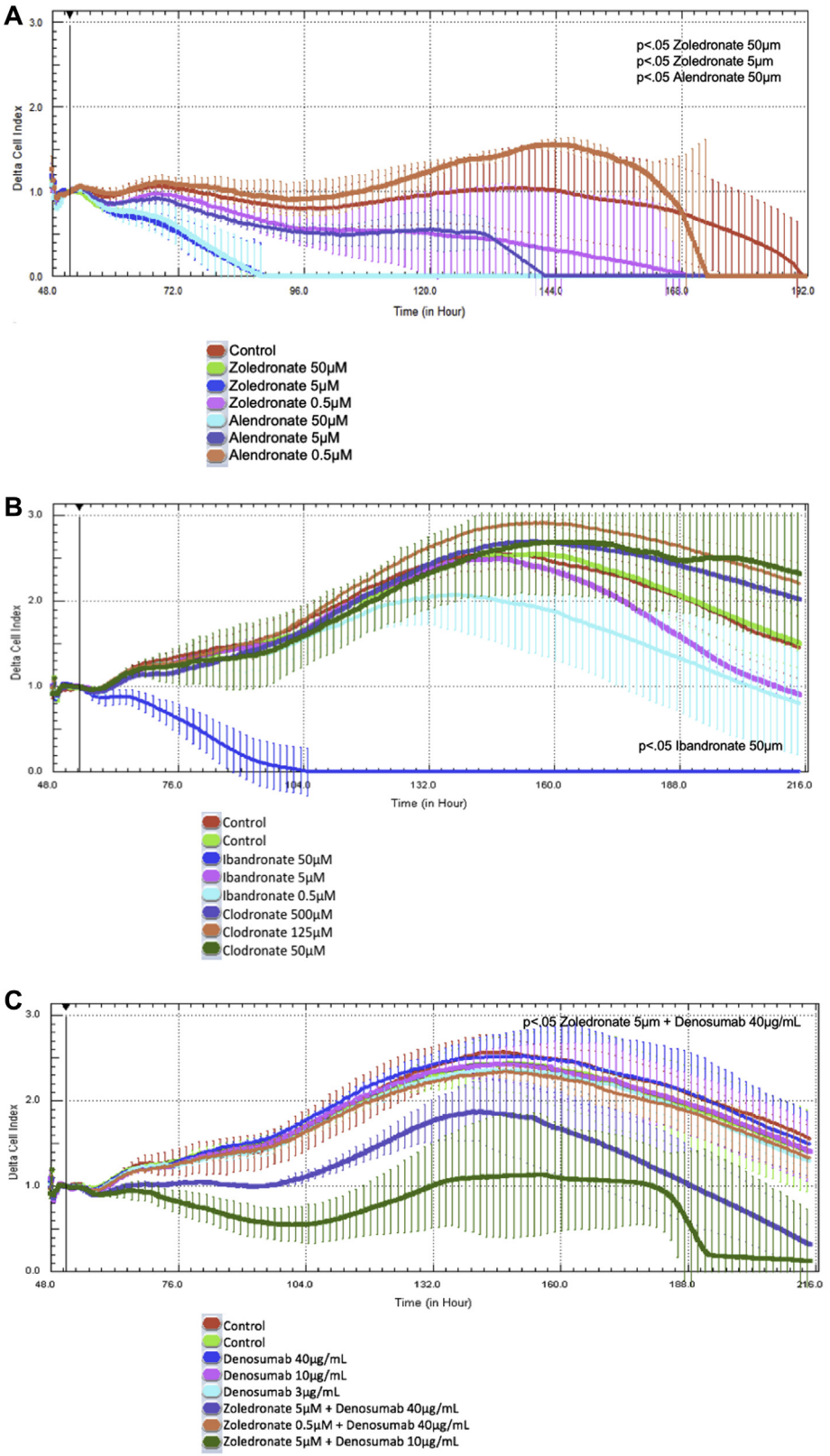

Fig. 3. Real-time monitoring of human gingival fibroblast cell adherence after confluence and exposure to Porphyromonas gingivalis lipopolysaccharide 10 µg/mL and antiresorptive medications at various concentrations in co-culture with THP-1 cells in an xCELLigence 0.4 µM porous ThinCert™. Cell curve describes the mean values of cell impedance and standard deviation up to 190 h of observation for the adherence curves of controls and (A) zoledronate and alendronate at concentrations of 0.5 µM, 5 µM, and 50 µM (B) clodronate at concentrations of 50 µM, 125 µM, and 500 µM and ibandronate at concentrations of 0.5 µM, 5 µM, and 50 µM, (C) denosumab at concentrations of 3 µg/mL, 10 µg/mL, and 40 µg/mL and combination of zoledronate and denosumab at concentrations of zoledronate 5 µM + denosumab 40 µg/mL, zoledronate 0.5 µM + denosumab 40 µg/mL, and zoledronate 5 µM + denosumab 10 µg/mL. Curve interruption is caused by medium renewal.

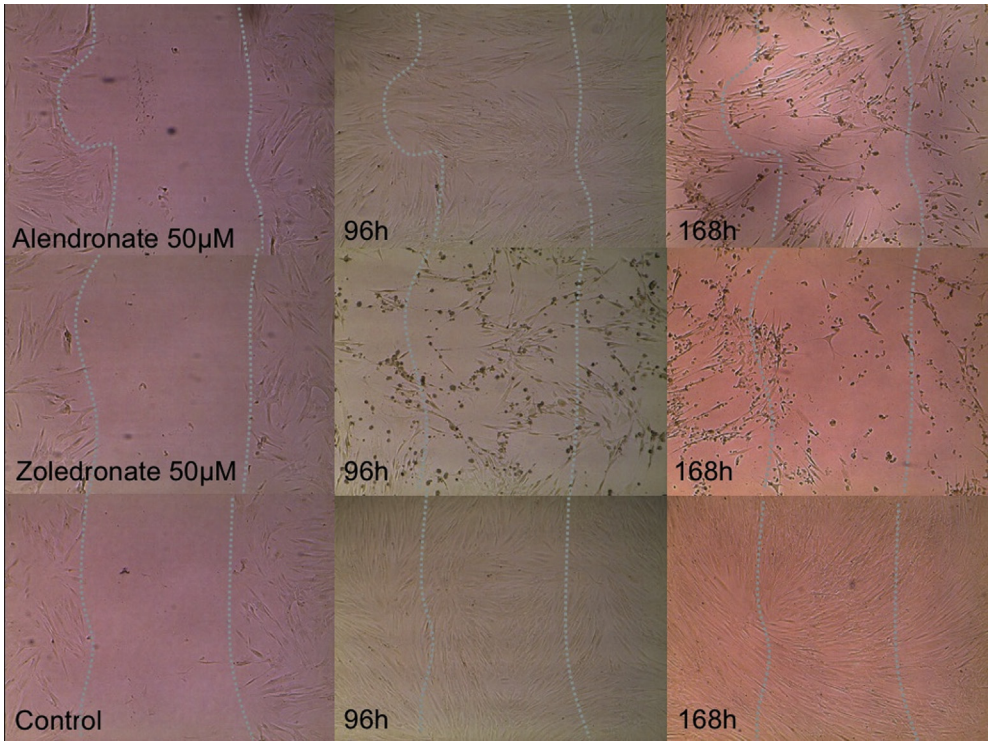

Fig. 4. Human gingival fibroblasts exposed to alendronate 50 μM, zoledronate 50 μM, or control in 24-well plate scratch assays at 0, 96, and 168 h after scratch and antiresorptive addition.

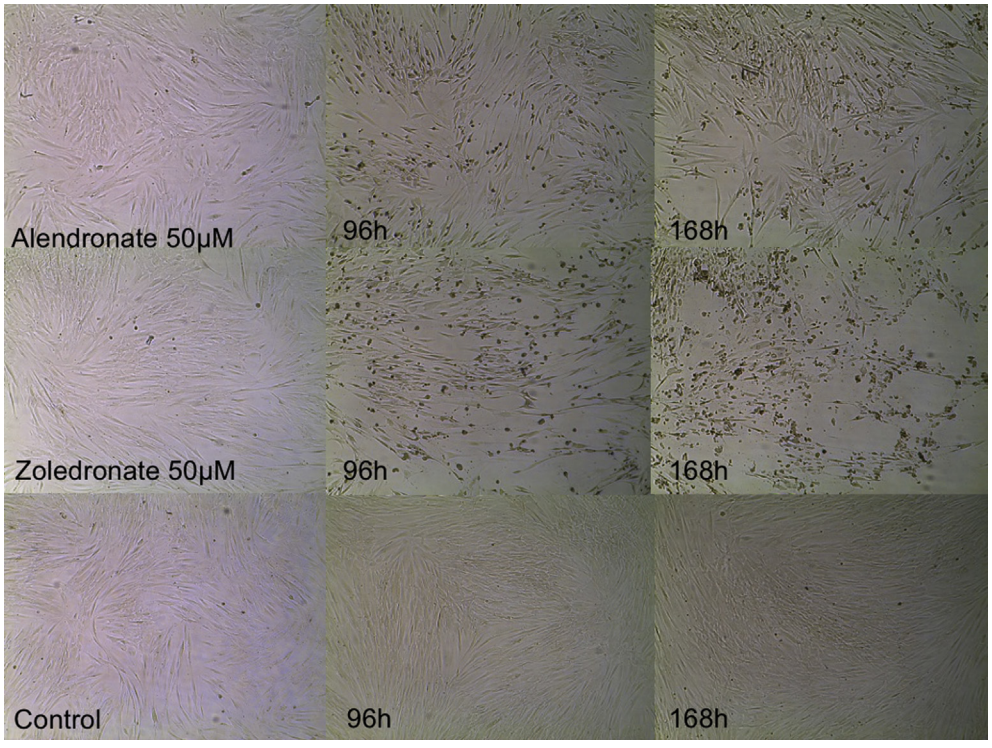

Fig. 5. Human gingival fibroblasts exposed to alendronate 50 μM with lipopolysaccharide (LPS), zoledronate 50 μM with LPS, or control in 24-well plates at 0, 96, and 168 h after antiresorptive addition.

small GTP-binding proteins Ras, Rho, Rac, and Rap, which are involved in a number of signaling pathways for cell migration and metabolism (Walker and Olson, 2005; Soydan et al., 2015). BP-induced disruption of HGF was rescued by the administration of geranylgeraniol in vitro (Cozin et al., 2011; Ziebart et al., 2011; Zafar et al., 2014).

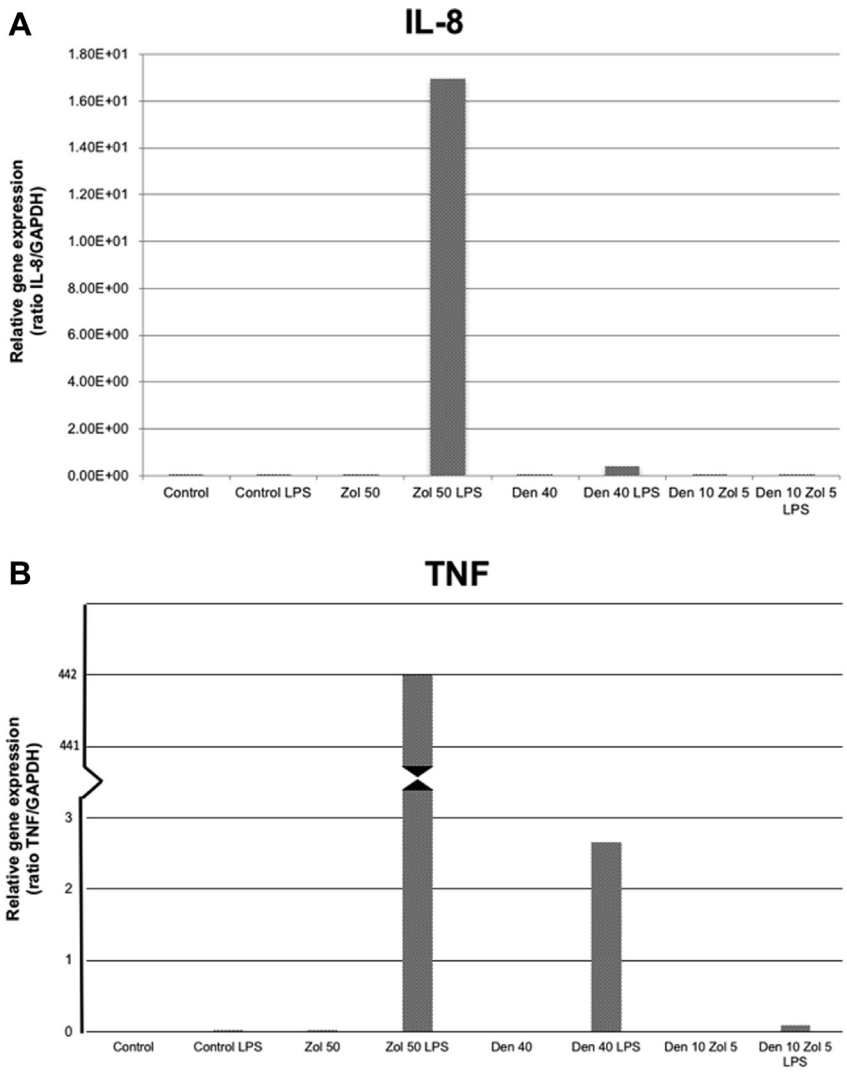

Fig. 6. (A) Relative gene expression of IL-8 and (B) TNFα with and without lipopolysaccharide. LPS = lipopolysaccharide; Zol = zoledronate; Den = denosumab.

Impaired wound healing was observed in the scratch assay with BPs as well as a combination of zoledronate and denosumab. Delayed wound healing due to zoledronate, pamidronate, and ibandronate (Walter et al., 2010) has been attributed to a down-regulation of type-I collagen transcription necessary to deposit granulation tissue needed for re-epithelization (Simon et al., 2010; Ravosa et al., 2011) Komatsu et al. also reported a reduction of type-I collagen expression via transforming growth factor beta (TGF-β) suppression in HGFs and proposed that impaired fibrous tissue formation could be due to Smad-dependent signal transduction inhibition (Komatsu et al., 2016). Diminished keratinocyte growth factor production by HGFs has also been suggested as a mechanism of delayed healing (Mawardi et al., 2011).

Our results demonstrated that antiresorptives were toxic to HGFs even without mechanical damage, particularly with the addition of LPS. Due to the periodontal anatomy, contact between BPs and the soft tissues is likely to occur in the absence of invasive dental surgery. Scheper et al. reported low levels of zoledronate released from bone, which may induce soft tissue apoptosis and inhibit proliferation (Scheper et al., 2010). Spontaneous incidences of necrosis without dental extraction (up to 42%) have been reported in MRONJ patients (Ruggiero and Kohn, 2015). This may explain sites of necrosis with dental prostheses, which may result in mucosal cell death without direct trauma (Niibe et al., 2015).

The addition of LPS increased fibroblast death and impaired wound healing. Bacterial challenge has been associated with MRONJ risk (Hansen et al., 2007; Hallmer et al., 2017). A mouse model exhibited unhealed gingival epithelium and delayed bone regeneration after tooth extraction and 15 days of pamidronate 1 mg/kg and Fusobacterium nucleatum (F. nucleatum) (Mawardi et al., 2011). The accompanying in vitro study also demonstrated significantly more fibroblast apoptosis when exposed to pamidronate and F. nucleatum compared to only BP, only bacteria, or control. Zoledronate 1–10 μM has been documented to promote the adherence of Streptococcus mutans to hydroxyapatite (Kobayashi et al., 2010). This is supported by clinical studies where BRONJ frequency is decreased with the elimination of bacteria-permeated dental plaque and antibiotic administration before dental surgery (Montefusco et al., 2008; Dimopoulos et al., 2009; Ripamonti et al., 2009). Since necrotic bone lesions have been reported to contain mainly anaerobic bacteria, intensified periodontitis control may be considered (Hansen et al., 2007; Sedghizadeh et al., 2008). Previous research has indicated that patients treated with BPs exhibited more P. gingivalis species than with denosumab, suggesting a role

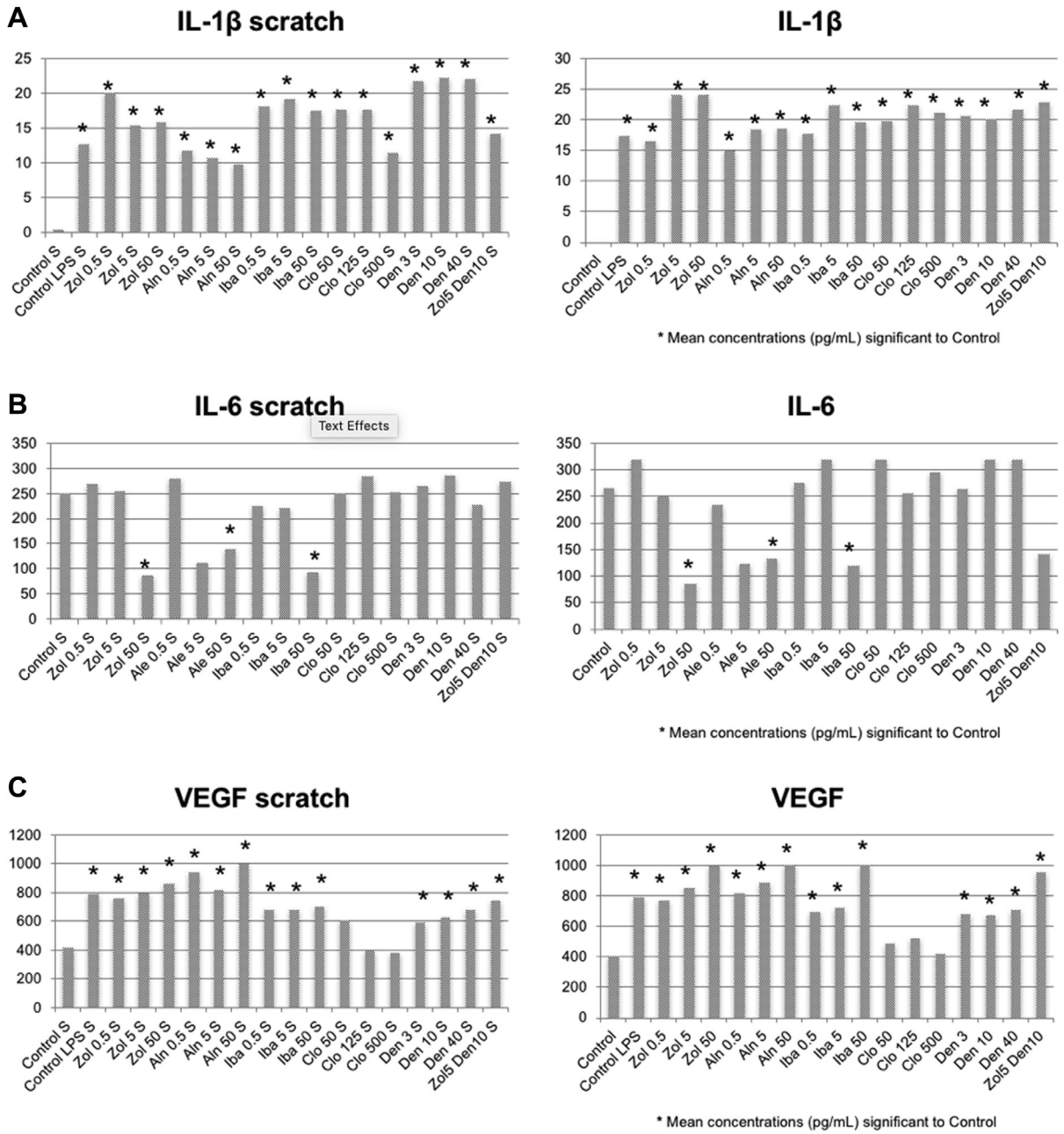

Fig. 7. (A) IL-1β concentrations of with and without scratch. (B) IL-6 concentrations with and without scratch. (C) VEGF concentrations with and without scratch. LPS = lipopolysaccharide; Zol = zoledronate; Aln = alendronate; Iba = ibandronate; Clo = clodronate; Den = denosumab.

of BPs in inducing an optimal environment for periopathogenic bacteria (Hallmer et al., 2017).

These results are one of the first to address the effect of combined therapy, which simulated the clinical setting with patients who have received BPs before initiating denosumab. Since the half-life of BPs could be ten years (Ravosa et al., 2011), it is realistic for patients to have residual BP effects while receiving denosumab. Zoledronate combined with denosumab demonstrated severe cell death even without mechanical damage and impaired wound healing, which was not observed with the denosumab-only group. There may be an influence of BP on HGFs which may be different from denosumab alone. The pharmacologic action of bisphosphonates is distinct from that of denosumab, since the former affects osteoclast function and the latter targets RANKL to cause the loss of osteoclasts (Baron et al., 2011). In our experiments with gingival fibroblasts, we observed that the expression of RANKL by HGFs was, as expected, not increased. However, high doses of zoledronate with LPS (and slightly with denosumab) elevated the expression of OPG. This could indicate that fibroblast signaling in osteoclastic bone remodeling is suppressed more by bisphosphonates than denosumab, particularly in the presence of bacteria. Previous studies also confirmed the increased expression of OPG and decreased RANKL with bisphosphonates, and the effects were exacerbated with LPS(Tipton et al., 2011).

Our experiments also present some of the first results on the singular effect of denosumab on HGFs, which inhibited wound healing at high concentrations but did not dismantle the fibroblast layer. Oral soft tissue toxicity was previously not reported with

denosumab (Ruggiero et al., 2014). A murine model demonstrated that denosumab administration resulted in a significant increase in CD3 and gamma delta (γδ) T cells locally, which may suggest a relationship between denosumab and inflammation and delayed connective tissue repair (Kuroshima et al., 2016). We observed an increase in TNFα expression, and it has been noted that γδ T cells cause a release in TNFα and the initiation of the acute phase inflammatory response (Thompson and Rogers, 2004).

Our experiments revealed elevated levels of IL-1β, TNFα, and IL-8 and decreased levels of IL-6 with antiresorptive exposure. Previous research demonstrated an increased production of proinflammatory cytokines IL-1, IL-6, and TNFα in active periodontitis (Trevani et al., 2003); these cytokines are also elevated in oral mucositis (Sonis, 2007). It was proposed that the overproduction of IL-1 and TNFα is closely linked to inflammation due to their regulation of COX-2 expression, resulting in the production of key inflammatory mediators (De Colli et al., 2015). The loss of fibroblasts that occurs during infection with periodontal pathogens is mediated by TNFα(Graves and Cochran, 2003), and periodontal destruction may represent an overreaction of the host response caused by excessive production of IL-1 and TNFα(Graves and Cochran, 2003). In murine models, BRONJ was seen to be associated with severe inflammation and immunosuppression (Sonis et al., 2009; Lopez-Jornet et al., 2011).

IL-6 is an important regulator of the immune system present in healthy patients and increased in a periodontal disease state (Matsuki et al., 1992). IL-6 plays a major role in B cell differentiation in the adaptive immune response (Takahashi et al., 1994). The decrease of IL-6 observed with high concentrations of aminobisphosphonates could suggest a dysfunction in the normal immune response. Since we observed elevated levels of IL-6 for every concentration except for most toxic concentrations of nitrogen-containing BPs, it could be conceivable that HGFs remain in the initial inflammatory stage, unable to activate the acquired immune system and resolve inflammation.

We did not observe any evidence of decreased angiogenesis, as there were elevated levels of VEGF and IL-8. Anti-angiogenic properties of antiresorptives have been often proposed as a mechanism for MRONJ (Wood et al., 2002; Santini et al., 2003a, 2003b; Giraudo et al., 2004). A reduction of blood vessels (Migliorati et al., 2005), inhibition of vascular endothelial cell proliferation and migration (Lang et al., 2016), as well as incorrect processing of VEGF-receptor 2 has been reported with MRONJ (Basi et al., 2010). However, other in vivo studies have also failed to demonstrate a strong relationship between BPs and reduced angiogenesis (Deckers et al., 2002; Santini et al., 2002). In fact, several groups have reported an upregulation of VEGF-A and bone morphogenetic protein 2 (BMP-2) gene expression, suggesting that fibroblasts respond to zoledronate by producing a proangiogenic environment (Zafar et al., 2014; Ohlrich et al., 2016). Tseng et al. reported IL-8 levels were significantly upregulated with zoledronate. An increased vascular flow could even permit more BPs to enter and accumulate in the bone and extracellular fluid (Burr and Allen, 2009).

A major limitation of our experiments was that although we attempted to account for the interactions of HGFs in co-culture, it would be ideal to observe the comprehensive interactions of the epithelium, connective tissue, and underlying bone in response to antiresorptives. A 3-dimensional model could be considered for future studies. The oncologic nature of the THP-1 cell used in co-culture may also have some limitations which could have contributed to fluctuations in measurement; future studies may consider isolated human monocytes. Further analyses to clarify the influence of IL-6 in vivo is also recommended, since results observed in vitro may not always translate to the clinical setting.

5. Conclusion

As the current patient population ages, clinicians may see an increase in MRONJ. Newer cases are being reported with other medication classes (Guarneri et al., 2010; Hoefert and Eufinger, 2010), and the use of potent BPs to treat osteoporosis is increasing in practice (Black et al., 2007). We propose that the etiology of MRONJ could be attributed to a combined intrinsic and extrinsic pathway of toxicity which includes soft tissue toxicity, altered immune response, and bacterial infiltration as key components. The anatomy of the oral mucosa with no fat or fascia barrier from underlying bone in combination with forces of daily jaw movement and sustained bacterial exposure could explain why these lesions are not present elsewhere. This was the first investigation of HGFs in real-time as well as the first study of denosumab and the combination of BP and denosumab in investigations of soft tissue in vitro. Our results suggest that MRONJ pathogenesis due to BPs versus denosumab may develop via differing mechanisms of action in the connective tissue layer resulting in similar presentations of underlying bone exposure.

Conflicts of Interest

No conflicts of interest declared for all authors.

Acknowledgements

This study was financially supported by the Forschungsgemeinschaft Dental e.V./Dental Research Society of Germany [grant number 02/2015].

The funding source had no role in study design, the collection, analysis and interpretation of data, writing of the report, and in the decision to submit the article for publication.

References

Acil Y, Moller B, Niehoff P, Rachko K, Gassling V, Wiltfang J, et al: The cytotoxic effects of three different bisphosphonates in-vitro on human gingival fibroblasts, osteoblasts and osteogenic sarcoma cells. J Cranio-Maxillo-Fac Surg: Off Publ Eur Assoc Cranio-Maxillo-Fac Surg 40: e229–e235, 2012

Baek KJ, Choi Y, Ji S: Gingival fibroblasts from periodontitis patients exhibit inflammatory characteristics in vitro. Arch Oral Biol 58: 1282–1292, 2013

Baron R, Ferrari S, Russell RG: Denosumab and bisphosphonates: different mechanisms of action and effects. Bone 48: 677–692, 2011

Basi DL, Lee SW, Helfman S, Mariash A, Lunos SA: Accumulation of VEGFR2 in zoledronic acid-treated endothelial cells. Mol Med Rep 3: 399–403, 2010

Bekker PJ, Holloway DL, Rasmussen AS, Murphy R, Martin SW, Leese PT, et al: A single-dose placebo-controlled study of AMG 162, a fully human monoclonal antibody to RANKL, in postmenopausal women. J Bone Miner Res: Off J Am Soc Bone Miner Res 19: 1059–1066, 2004

Black DM, Delmas PD, Eastell R, Reid IR, Boonen S, Cauley JA, et al: Once-yearly zoledronic acid for treatment of postmenopausal osteoporosis. New Engl J Med 356: 1809–1822, 2007

Burr DB, Allen MR: Mandibular necrosis in beagle dogs treated with bisphosphonates. Orthod Craniofac Res 12: 221–228, 2009

Cozin M, Pinker BM, Solemani K, Zuniga JM, Dadaian SC, Cremers S, et al: Novel therapy to reverse the cellular effects of bisphosphonates on primary human oral fibroblasts. J Oral Maxillofac Surg: Off J Am Assoc Oral Maxillofac Surg 69: 2564–2578, 2011

De Colli M, Zara S, di Giacomo V, Patruno A, Marconi GD, Gallorini M, et al: Nitric oxide-mediated cytotoxic effect induced by zoledronic acid treatment on human gingival fibroblasts. Clin Oral Investig 19: 1269–1277, 2015

Deckers MM, Van Beek ER, Van Der Pluijm G, Wetterwald A, Van Der Wee-Pals L, Cecchini MG, et al: Dissociation of angiogenesis and osteoclastogenesis during endochondral bone formation in neonatal mice. J Bone Miner Res: Off J Am Soc Bone Miner Res 17: 998–1007, 2002

Dimopoulos MA, Kastritis E, Bamia C, Melakopoulos I, Gika D, Roussou M, et al: Reduction of osteonecrosis of the jaw (ONJ) after implementation of preventive measures in patients with multiple myeloma treated with zoledronic acid. Ann Oncol: Off J Eur Soci Med Oncol/ESMO 20: 117–120, 2009

Fu Q, Cui C, Xuan B, Guo Y, Liu C, Zhang J: Effect of zoledronic acid on cell proliferation and apoptosis of human periodontal fibroblasts. Zhonghua Kou Qiang Yi Xue Za Zhi 50: 667–670, 2015

Giraudo E, Inoue M, Hanahan D: An amino-bisphosphonate targets MMP-9-expressing macrophages and angiogenesis to impair cervical carcinogenesis. J Clin Invest 114: 623–633, 2004
Graves DT, Cochran D: The contribution of interleukin-1 and tumor necrosis factor to periodontal tissue destruction. J Periodontol 74: 391–401, 2003
Guarneri V, Miles D, Robert N, Dieras V, Glaspy J, Smith I, et al: Bevacizumab and osteonecrosis of the jaw: incidence and association with bisphosphonate therapy in three large prospective trials in advanced breast cancer. Breast Canc Res Treat 122: 181–188, 2010
Hallmer F, Bjornland T, Andersson G, Becktor JP, Kristoffersen AK, Enersen M: Bacterial diversity in medication-related osteonecrosis of the jaw. J Oral Med Oral Surg Oral Pathol Oral Radiol 123: 436–444, 2017
Hansen T, Kunkel M, Springer E, Walter C, Weber A, Siegel E, et al: Actinomycosis of the jaws–histopathological study of 45 patients shows significant involvement in bisphosphonate-associated osteonecrosis and infected osteoradionecrosis. Virchows Arch 451: 1009–1017, 2007
Hoefert S, Eufinger H: Sunitinib may raise the risk of bisphosphonate-related osteonecrosis of the jaw: presentation of three cases. Oral Surg Oral Med Oral Pathol Oral Radiol Endod 110: 463–469, 2010
Hoefert S, Sade Hoefert C, Munz A, Schmitz I, Grimm M, Yuan A, et al: Effect of bisphosphonates on macrophagic THP-1 cell survival in bisphosphonate-related osteonecrosis of the jaw (BRONJ). J Oral Med Oral Surg Oral Pathol Oral Radiol 121: 222–232, 2016
Kobayashi Y, Hiraga T, Ueda A, Wang L, Matsumoto-Nakano M, Hata K, et al: Zoledronic acid delays wound healing of the tooth extraction socket, inhibits oral epithelial cell migration, and promotes proliferation and adhesion to hydroxyapatite of oral bacteria, without causing osteonecrosis of the jaw, in mice. J Bone Miner Metab 28: 165–175, 2010
Komatsu Y, Ibi M, Chosa N, Kyakumoto S, Kamo M, Shibata T, et al: Zoledronic acid suppresses transforming growth factor-beta-induced fibrogenesis by human gingival fibroblasts. Int J Mol Med 38: 139–147, 2016
Kuroshima S, Al-Salihi Z, Yamashita J: Mouse anti-RANKL antibody delays oral wound healing and increases TRAP-positive mononuclear cells in bone marrow. Clin Oral Investig 20: 727–736, 2016
Landesberg R, Cozin M, Cremers S, Woo V, Kousteni S, Sinha S, et al: Inhibition of oral mucosal cell wound healing by bisphosphonates. J Oral Maxillofac Surg: Off J Am Assoc Oral Maxillofaci Surg 66: 839–847, 2008
Lang M, Zhou Z, Shi L, Niu J, Xu S, Lin W, et al: Influence of zoledronic acid on proliferation, migration, and apoptosis of vascular endothelial cells. Br J Oral Maxillofac Surg 54: 889–893, 2016
Lopez-Jornet P, Camacho-Alonso F, Martinez-Canovas A, Molina-Minano F, Gomez-Garcia F, Vicente-Ortega V: Perioperative antibiotic regimen in rats treated with pamidronate plus dexamethasone and subjected to dental extraction: a study of the changes in the jaws. J Oral Maxillofac Surg: Off J Am Assoc Oral Maxillofaci Surg 69: 2488–2493, 2011
Marx RE: Pamidronate (Aredia) and zoledronate (Zometa) induced avascular necrosis of the jaws: a growing epidemic. J Oral Maxillofac Surg: Off J Am Assoc Oral Maxillofaci Surg 61: 1115–1117, 2003
Matsuki Y, Yamamoto T, Hara K: Detection of inflammatory cytokine messenger RNA (mRNA)-expressing cells in human inflamed gingiva by combined in situ hybridization and immunohistochemistry. Immunology 76: 42–47, 1992
Mawardi H, Giro G, Kajiya M, Ohta K, Almazrooa S, Alshwaimi E, et al: A role of oral bacteria in bisphosphonate-induced osteonecrosis of the jaw. J Dent Res 90: 1339–1345, 2011
Migliorati CA, Schubert MM, Peterson DE, Seneda LM: Bisphosphonate-associated osteonecrosis of mandibular and maxillary bone: an emerging oral complication of supportive cancer therapy. Cancer 104: 83–93, 2005
Monkkonen J, Koponen HM, Ylitalo P: Comparison of the distribution of three bisphosphonates in mice. Pharmacol Toxicol 66: 294–298, 1990
Montefusco V, Gay F, Spina F, Miceli R, Maniezzo M, Teresa Ambrosini M, et al: Antibiotic prophylaxis before dental procedures may reduce the incidence of osteonecrosis of the jaw in patients with multiple myeloma treated with bisphosphonates. Leuk Lymphoma 49: 2156–2162, 2008
Niibe K, Ouchi T, Iwasaki R, Nakagawa T, Horie N: Osteonecrosis of the jaw in patients with dental prostheses being treated with bisphosphonates or denosumab. J Prosthodont Res 59: 3–5, 2015
Ohlrich EJ, Coates DE, Cullinan MP, Milne TJ, Zafar S, Zhao Y, et al: The bisphosphonate zoledronic acid regulates key angiogenesis-related genes in primary human gingival fibroblasts. Arch Oral Biol 63: 7–14, 2016
Ravosa MJ, Ning J, Liu Y, Stack MS: Bisphosphonate effects on the behaviour of oral epithelial cells and oral fibroblasts. Arch Oral Biol 56: 491–498, 2011
Reid IR, Bolland MJ, Grey AB: Is bisphosphonate-associated osteonecrosis of the jaw caused by soft tissue toxicity? Bone 41: 318–320, 2007
Ripamonti CI, Maniezzo M, Campa T, Fagnoni E, Brunelli C, Saibene G, et al: Decreased occurrence of osteonecrosis of the jaw after implementation of dental preventive measures in solid tumour patients with bone metastases treated with bisphosphonates. The experience of the National Cancer Institute of Milan. Ann Oncol: Off J Eur Soc Med Oncol/ESMO 20: 137–145, 2009
Ruggiero SL, Dodson TB, Fantasia J, Goodday R, Aghaloo T, Mehrotra B, et al: American Association of Oral and Maxillofacial Surgeons position paper on medication-related osteonecrosis of the jaw–2014 update. J Oral Maxillofac Surg: Off J Am Assoc Oral Maxillofac Surg 72: 1938–1956, 2014
Ruggiero SL, Kohn N: Disease stage and mode of therapy are important determinants of treatment outcomes for medication-related osteonecrosis of the jaw. J Oral Maxillofac Surg: Off J Am Assoc Oral Maxillofac Surg 73: S94–S100, 2015
Santini D, Vespasiani Gentilucci U, Vincenzi B, Picardi A, Vasaturo F, La Cesa A, et al: The antineoplastic role of bisphosphonates: from basic research to clinical evidence. Ann Oncol: Off J Eur Soc Med Oncol/ESMO 14: 1468–1476, 2003a
Santini D, Vincenzi B, Avvisati G, Dicuonzo G, Battistoni F, Gavasci M, et al: Pamidronate induces modifications of circulating angiogenetic factors in cancer patients. Clin Cancer Res: Off J Am Assoc Cancer Res 8: 1080–1084, 2002
Santini D, Vincenzi B, Dicuonzo G, Avvisati G, Massacesi C, Battistoni F, et al: Zoledronic acid induces significant and long-lasting modifications of circulating angiogenic factors in cancer patients. Clin Cancer Res: Off J Am Assoc Cancer Res 9: 2893–2897, 2003b
Scheper M, Chaisuparat R, Cullen K, Meiller T: A novel soft-tissue in vitro model for bisphosphonate-associated osteonecrosis. Fibrogenesis Tissue Repair 3: 6, 2010
Scheper MA, Badros A, Chaisuparat R, Cullen KJ, Meiller TF: Effect of zoledronic acid on oral fibroblasts and epithelial cells: a potential mechanism of bisphosphonate-associated osteonecrosis. Br J Haematol 144: 667–676, 2009
Sedghizadeh PP, Kumar SK, Gorur A, Schaudinn C, Shuler CF, Costerton JW: Identification of microbial biofilms in osteonecrosis of the jaws secondary to bisphosphonate therapy. J Oral Maxillofac Surg: Off J Am Assoc Oral Maxillofac Surg 66: 767–775, 2008
Simon MJ, Niehoff P, Kimmig B, Wiltfang J, Acil Y: Expression profile and synthesis of different collagen types I, II, III, and V of human gingival fibroblasts, osteoblasts, and SaOS-2 cells after bisphosphonate treatment. Clin Oral Investig 14: 51–58, 2010
Sonis ST: Pathobiology of oral mucositis: novel insights and opportunities. J Support Oncol 5: 3–11, 2007
Sonis ST, Watkins BA, Lyng GD, Lerman MA, Anderson KC: Bony changes in the jaws of rats treated with zoledronic acid and dexamethasone before dental extractions mimic bisphosphonate-related osteonecrosis in cancer patients. Oral Oncology 45: 164–172, 2009
Soydan SS, Araz K, Senel FV, Yurtcu E, Helvacioglu F, Dagdeviren A, et al: Effects of alendronate and pamidronate on apoptosis and cell proliferation in cultured primary human gingival fibroblasts. Hum Exp Toxicol 34: 1073–1082, 2015
Suthin K, Matsushita K, Machigashira M, Tatsuyama S, Imamura T, Torii M, et al: Enhanced expression of vascular endothelial growth factor by periodontal pathogens in gingival fibroblasts. J Periodontal Res 38: 90–96, 2003
Takahashi K, Takashiba S, Nagai A, Takigawa M, Myoukai F, Kurihara H, et al: Assessment of interleukin-6 in the pathogenesis of periodontal disease. J Periodontol 65: 147–153, 1994
Thompson K, Rogers MJ: Statins prevent bisphosphonate-induced gamma,delta-T-cell proliferation and activation in vitro. J Bone Miner Res: Off J Am Soc Bone Miner Res 19: 278–288, 2004
Tipton DA, Seshul BA, Dabbous M: Effect of bisphosphonates on human gingival fibroblast production of mediators of osteoclastogenesis: RANKL, osteoprotegerin and interleukin-6. J Periodontal Res 46: 39–47, 2011
Trevani AS, Chorny A, Salamone G, Vermeulen M, Gamberale R, Schettini J, et al: Bacterial DNA activates human neutrophils by a CpG-independent pathway. Eur J Immunol 33: 3164–3174, 2003
Walker K, Olson MF: Targeting Ras and Rho GTPases as opportunities for cancer therapeutics. Curr Opin Genet Dev 15: 62–68, 2005
Walter C, Al-Nawas B, Grotz KA, Thomas C, Thuroff JW, Zinser V, et al: Prevalence and risk factors of bisphosphonate-associated osteonecrosis of the jaw in prostate cancer patients with advanced disease treated with zoledronate. Eur Urol 54: 1066–1072, 2008
Walter C, Klein MO, Pabst A, Al-Nawas B, Duschner H, Ziebart T: Influence of bisphosphonates on endothelial cells, fibroblasts, and osteogenic cells. Clin Oral Investig 14: 35–41, 2010
Walter C, Pabst A, Ziebart T, Klein M, Al-Nawas B: Bisphosphonates affect migration ability and cell viability of HUVEC, fibroblasts and osteoblasts in vitro. Oral Dis 17: 194–199, 2011
Wood J, Bonjean K, Ruetz S, Bellahcene A, Devy L, Foidart JM, et al: Novel anti-angiogenic effects of the bisphosphonate compound zoledronic acid. J Pharmacol Exp Ther 302: 1055–1061, 2002
Zafar S, Coates DE, Cullinan MP, Drummond BK, Milne T, Seymour GJ: Zoledronic acid and geranylgeraniol regulate cellular behaviour and angiogenic gene expression in human gingival fibroblasts. J Oral Pathol Med: Off Publ Int Assoc Oral Pathol Am Acad Oral Pathol 43: 711–721, 2014
Ziebart T, Koch F, Klein MO, Guth J, Adler J, Pabst A, et al: Geranylgeraniol - a new potential therapeutic approach to bisphosphonate associated osteonecrosis of the jaw. Oral Oncol 47: 195–201, 2011